1304 *Inorg. Chem.* **2011**, *50*, 1304–1308
DOI: 10.1021/ic101849h

Inorganic Chemistry
Article

Heterometallic Cubanes: Syntheses, Structures, and Magnetic Properties of Lanthanide(III)−Nickel(II) Architectures

Yajie Gao,[†,‡] Lang Zhao,[†] Xuebin Xu,[†,‡] Gong-Feng Xu,[†] Yun-Nan Guo,[†,§] Jinkui Tang,[*,†] and Zhiliang Liu[‡]

[†]*State Key Laboratory of Rare Earth Resource Utilization, Changchun Institute of Applied Chemistry, Chinese Academy of Sciences, Changchun 130022, People's Republic of China,* [‡]*College of Chemistry and Chemical Engineering, Inner Mongolia University, Hohhot 010021, People's Republic of China, and* [§]*Graduate School of the Chinese Academy of Sciences, Beijing, 100039, People's Republic of China*

Received September 9, 2010

Reactions of lanthanide(III) perchlorate (Ln = Dy, Tb, and Gd), nickel(II) acetate, and ditopic ligand 2-(benzothiazol-2-ylhydrazonomethyl)-6-methoxyphenol (**H_2L**) in a mixture of methanol and acetone in the presence of NaOH resulted in the successful assembly of novel Ln_2Ni_2 heterometallic clusters representing a new heterometallic 3d−4f motif. Single-crystal X-ray diffraction reveals that all compounds are isostructural, with the central core composed of distorted $[Ln_2Ni_2O_4]$ cubanes of the general formula $[Ln_2Ni_2(\mu_3\text{-}OH)_2(OH)(OAc)_4(HL)_2(MeOH)_3](ClO_4)\cdot 3MeOH$ [Ln = Dy (**1**), Tb (**2**), and Gd (**3**)]. The magnetic properties of all compounds have been investigated. Magnetic analysis on compound **3** indicates ferromagnetic Gd···Ni exchange interactions competing with antiferromagnetic Ni···Ni interactions. Compound **1** displays slow relaxation of magnetization, which is largely attributed to the presence of the anisotropic Dy^{III} ions, and thus represents a new discrete $[Dy_2Ni_2]$ heterometallic cubane exhibiting probable single-molecule magnetic behavior.

Introduction

Since the discovery of single-molecule magnets (SMMs), much effort has been focused on the preparation of new molecular aggregates possessing both high spin and anisotropy.[1] In this context, metallic cubanes are highly promising systems for the development of high-spin molecules because quite often ferromagnetic exchange coupling and high-spin ground state can be expected. Indeed, many such compounds have been reported for 3d elements.[2] Compared to 3d transition metals, lanthanide ions are especially often characterized by large spin values and the presence of strong Ising-type magnetic anisotropy because of their important spin−orbit coupling.[3] Thus, it has been of interest to modify the structure of the cubane compound by introducing one or more lanthanide ions into the cluster. Such a modification may affect the magnetic anisotropy, spin ground state, and magnetic exchange interactions within metal clusters, thus providing a means of understanding the different magnetic contributions to the SMM behavior encountered in 3d−4f compounds.[2f,4]

Along this strategy and starting from a tetranuclear copper(II) compound with a cubane-like structure, Luneau and co-workers have successfully isolated two series of heterobimetallic $Ln^{III}-Cu^{II}$ tetranuclear $[LnCu_3]$ and nonanuclear $[Ln_3Cu_6]$ clusters by replacing one or two of the Cu^{II} ions in the parent compound by lanthanide ions.[2f,4] Among them, a $[Dy_3Cu_6]$ cluster, which can be viewed as resulting from the fusion of three Dy_2Cu_2 cubane cores sharing the lanthanide ions in a triangular fashion, behaves as an SMM with a strong coercive field.[4] $[Mn_2Dy_2]$[5] and $[Gd_3Fe]$[6] have

*To whom correspondence should be addressed. E-mail: tang@ciac.jl.cn.

(1) (a) Tasiopoulos, A. J.; Vinslava, A.; Wernsdorfer, W.; Abboud, K. A.; Christou, G. *Angew. Chem., Int. Ed.* **2004**, *43*, 2117–2121. (b) Ako, A. M.; Hewitt, I. J.; Mereacre, V.; Clérac, R.; Wernsdorfer, W.; Anson, C. E.; Powell, A. K. *Angew. Chem., Int. Ed.* **2006**, *45*, 4926–4929. (c) Aromı́, G.; Brechin, E. K. *Struct. Bonding* (*Berlin*) **2006**, *122*, 1–67. (d) Gatteschi, D.; Sessoli, R.; Villain, J. *Molecular Nanomagnets*; Oxford University Press: Oxford, U.K., 2006. (e) Ako, A. M.; Mereacre, V.; Clérac, R.; Wernsdorfer, W.; Hewitt, I.; Anson, C. E.; Powell, A. K. *Chem. Commun.* **2009**, 544–546.

(2) (a) Aubin, S. M. J.; Wemple, M. W.; Adams, D. M.; Tsai, H.-L.; Christou, G.; Hendrickson, D. N. *J. Am. Chem. Soc.* **1996**, *118*, 7746–7754. (b) Oshio, H.; Hoshino, N.; Ito, T. *J. Am. Chem. Soc.* **2000**, *122*, 12602–12603. (c) Kessler, V. G.; Gohil, S.; Kritikos, M.; Korsak, O. N.; Knyazeva, E. E.; Moskovskaya, I. F.; Romanovsky, B. V. *Polyhedron* **2001**, *20*, 915–922. (d) Mukherjee, A.; Nethaji, M.; Chakravarty, A. R. *Angew. Chem., Int. Ed.* **2004**, *43*, 87–90. (e) Oshio, H.; Nihei, M.; Koizumi, S.; Shiga, T.; Nojiri, H.; Nakano, M.; Shirakawa, N.; Akatsu, M. *J. Am. Chem. Soc.* **2005**, *127*, 4568–4569. (f) Aronica, C.; Chastanet, G.; Pilet, G.; Le Guennic, B.; Robert, V.; Wernsdorfer, W.; Luneau, D. *Inorg. Chem.* **2007**, *46*, 6108–6119. (g) Feng, P. L.; Beedle, C. C.; Wernsdorfer, W.; Koo, C.; Nakano, M.; Hill, S.; Hendrickson, D. N. *Inorg. Chem.* **2007**, *46*, 8126–8128. (h) Feng, P. L.; Beedle, C. C.; Koo, C.; Wernsdorfer, W.; Nakano, M.; Hill, S.; Hendrickson, D. N. *Inorg. Chem.* **2008**, *47*, 3188–3204. (i) Stoumpos, C. C.; Gass, I. A.; Milios, C. J.; Lalioti, N.; Terzis, A.; Aromi, G.; Teat, S. J.; Brechin, E. K.; Perlepes, S. P. *Dalton Trans.* **2009**, 307–317. (j) Zhang, J.; Teo, P.; Pattacini, R.; Kermagoret, A.; Welter, R.; Rogez, G.; Hor, T.; Braunstein, P. *Angew. Chem., Int. Ed.* **2010**, *49*, 4443–4446.

(3) Sessoli, R.; Powell, A. K. *Coord. Chem. Rev.* **2009**, *253*, 2328–2341.

(4) Aronica, C.; Pilet, G.; Chastanet, G.; Wernsdorfer, W.; Jacquot, J. F.; Luneau, D. *Angew. Chem., Int. Ed.* **2006**, *45*, 4659–4662.

 Published on Web 01/21/2011

Scheme 1. Representation of the Ligand $\mathbf{H_2L}$

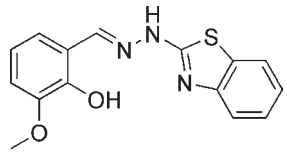

also been reported as substructures of larger polynuclear 3d−4f complexes, respectively. In addition, heterometallic 3d−4f cubane clusters [Cu_3Gd] have been found in polyoxometalate matrixes.[7] Very recently, [Co_2Ln_2] (Ln = Y, Gd, Tb, Dy, and Ho) compounds have been reported; of these compounds, [Co_2Dy_2] exhibits slow relaxation of magnetization, which is mainly due to the presence of the anisotropic Dy^{III} ions.[8]

Noting that Dy^{III} shows interesting magnetic behavior[9] and taking advantage of the Ni^{II} ion's significant single-ion anisotropy,[10] we intend to explore the possibility of obtaining a $Dy^{III}-Ni^{II}$ heterometallic cubane having 2-(benzothiazol-2-ylhydrazonomethyl)-6-methoxyphenol ($\mathbf{H_2L}$, Scheme 1) as the bifunctional ligand to combine the 3d and 4f centers. The readily prepared organic ligand $\mathbf{H_2L}$ has a rigid molecular structure with ditopic binding sites, capable of both coordinating and connecting the different types of metal ion centers. By using a mixture of nickel(II) and lanthanide(III) salts, we succeeded in synthesizing a family of heterometallic cubanes of the general formula $[Ln_2Ni_2(\mu_3\text{-}OH)_2(OH)(OAc)_4(HL)_2(MeOH)_3](ClO_4)\cdot 3MeOH$ [Ln = Dy (**1**), Tb (**2**), and Gd (**3**)]. Compound **1** represents a new discrete [Dy_2Ni_2] heterometallic cubane exhibiting probable SMM behavior, where its slow relaxation of magnetization is probably attributed to the presence of the anisotropic Dy^{III} ions. Magnetic analysis on compound **3** indicates a competition between ferromagnetic Gd···Ni exchange interactions and antiferromagnetic Ni···Ni interactions.

Experimental Section

All chemicals were of analytical reagent grade and were used as received. 2-Hydrazinobenzothiazole was prepared by a literature procedure described elsewhere.[11] The Schiff-base ligand was synthesized by a condensation reaction between 2-hydrazinobenzothiazole (0.165 g, 1 mmol) and *o*-vanillin (0.1673 g, 1.1 mmol) in methanol.

Synthesis of Dy_2Ni_2 (1). A solution of $\mathbf{H_2L}$ (44.8 mg, 0.15 mmol) in methanol/acetone (2:1, 15 mL) containing $Dy(ClO_4)_3\cdot 6H_2O$ (85.3 mg, 0.15 mmol) was stirred at 40 °C, while a freshly prepared methanol solution of NaOH (0.02 mL, 1.0 M) was added. After stirring for 4 h, $Ni(OAc)_2\cdot 4H_2O$ (24.8 mg, 0.1 mmol) was added to the resulting yellow solution. Then the mixture was stirred for another 1 h, followed by filtration. Brown single crystals suitable for X-ray structure analysis were formed at room temperature by slow evaporation of the filtrates. Yield: 38 mg (47% based on nickel acetate). Anal. Calcd (found) for $C_{44}H_{63}ClN_6O_{25}S_2Ni_2Dy_2$: C, 32.66 (32.76); N, 5.19 (5.23); H, 3.92 (3.77). IR [ν(CN), cm^{-1}]: 3422 (b), 1605 (m), 1570 (s), 1514 (w), 1451 (s), 1384 (w), 1269 (m), 1240 (m), 1225 (s), 1122 (s), 1081 (m), 940 (w), 743 (m), 637 (w).

Synthesis of Tb_2Ni_2 (2). This compound was prepared using the same procedure as that described above for the synthesis of its dysprosium(III) cognate but using $Tb(ClO_4)_3\cdot 6H_2O$ in place of $Dy(ClO_4)_3\cdot 6H_2O$. Yield: 36 mg (45% based on nickel acetate). Anal. Calcd (found) for $C_{44}H_{63}ClN_6O_{25}S_2Ni_2Tb_2$: C, 32.81 (32.72); N, 5.22 (5.49); H, 3.94 (3.67). IR [ν(CN), cm^{-1}]: 2943 (m), 1605 (m), 1571 (s), 1512 (m), 1383 (w), 1321 (w), 1269 (s), 1239 (s), 1223 (m), 1080 (s), 940 (s), 742 (s).

Synthesis of Gd_2Ni_2 (3). This compound was prepared using the same procedure as that described above for the synthesis of its dysprosium(III) cognate but using $Gd(ClO_4)_3\cdot 6H_2O$ in place of $Dy(ClO_4)_3\cdot 6H_2O$. Yield: 33 mg (41% based on nickel acetate). Anal. Calcd (found) for $C_{44}H_{63}ClN_6O_{25}S_2Ni_2Gd_2$: C, 32.88 (32.68); N, 5.23 (5.35); H, 3.95 (3.86). IR [ν(CN), cm^{-1}]: 2960 (m), 1605 (m), 1571 (s), 1514 (m), 1383 (w), 1269 (s), 1241 (s), 1224 (m), 1080 (s), 940 (s), 741 (s).

Physical Measurements. Elemental analysis for C, H, and N was carried out on a Perkin-Elmer 2400 analyzer. Fourier transform infrared (FTIR) spectra were recorded with a Vertex 70 FTIR spectrophotometer using the reflectance technique (4000−300 cm^{-1}). Samples were prepared as KBr disks. Magnetic susceptibility measurements were performed in the temperature range 2−300 K using a Quantum Design MPMS XL-7 SQUID magnetometer equipped with a 7 T magnet. The direct-current (dc) measurements were collected from 2 to 300 K, and the alternating-current (ac) measurements were carried out in a 3.0 Oe ac field oscillating at various frequencies from 100 to 1500 Hz and with or without a dc field. The diamagnetic corrections for the compounds were estimated using Pascal's constants,[12] and magnetic data were corrected for diamagnetic contributions of the sample holder.

Crystallography. Crystallographic data and refinement details are given in Table 1. Suitable single crystals with dimensions of $0.19\times 0.15\times 0.12$, $0.19\times 0.17\times 0.14$, and $0.19\times 0.17\times 0.14$ mm^3 for **1**−**3** respectively, were selected for single-crystal X-ray diffraction analysis. Crystallographic data were collected at a temperature of 186(2) K for **1** and **2** and 191(2) K for **3** on a Bruker ApexII CCD diffractometer with graphite-monochromated Mo Kα radiation (λ = 0.710 73 Å). Data processing was accomplished with the *SAINT* processing program.[13] The structure was solved by direct methods and refined on F^2 by full-matrix least squares using *SHELXTL*.[14] The location of metal atoms were easily determined, and oxygen, nitrogen, and carbon atoms were subsequently determined from the difference Fourier maps. The non-hydrogen atoms were refined anisotropically. The hydrogen atoms were introduced in calculated positions and refined with a fixed geometry with respect to their carrier atoms. CCDC 772946 (**1**), 772948 (**2**), and 772947 (**3**)

(5) Mereacre, V. M.; Ako, A. M.; Clérac, R.; Wernsdorfer, W.; Hewitt, I. J.; Anson, C. E.; Powell, A. K. *Chem.—Eur. J.* **2008**, *14*, 3577–3584.
(6) Ako, A. M.; Mereacre, V.; Clerac, R.; Hewitt, I. J.; Lan, Y. H.; Anson, C. E.; Powell, A. K. *Dalton Trans.* **2007**, 5245–5247.
(7) Nohra, B.; Mialane, P.; Dolbecq, A.; Riviere, E.; Marrot, J.; Secheresse, F. *Chem. Commun.* **2009**, 2703–2705.
(8) Zhao, X. Q.; Lan, Y. H.; Zhao, B.; Cheng, P.; Anson, C. E.; Powell, A. K. *Dalton Trans.* **2010**, *39*, 4911–4917.
(9) (a) Tang, J.; Hewitt, I.; Madhu, N. T.; Chastanet, G.; Wernsdorfer, W.; Anson, C. E.; Benelli, C.; Sessoli, R.; Powell, A. K. *Angew. Chem., Int. Ed.* **2006**, *45*, 1729–1733. (b) Gao, Y.; Xu, G.-F.; Zhao, L.; Tang, J.; Liu, Z. *Inorg. Chem.* **2009**, *48*, 11495–11497. (c) Savard, D.; Lin, P.-H.; Burchell, T. J.; Korobkov, I.; Wernsdorfer, W.; Clérac, R.; Murugesu, M. *Inorg. Chem.* **2009**, *48*, 11748–11754. (d) Ke, H.; Gamez, P.; Zhao, L.; Xu, G.-F.; Xue, S.; Tang, J. *Inorg. Chem.* **2010**, *49*, 7549–7557.
(10) (a) Rogez, G.; Rebilly, J. N.; Barra, A. L.; Sorace, L.; Blondin, G.; Kirchner, N.; Duran, M.; van Slageren, J.; Parsons, S.; Ricard, L.; Marvilliers, A.; Mallah, T. *Angew. Chem., Int. Ed.* **2005**, *44*, 1876–1879. (b) Stamatatos, T. C.; Abboud, K. A.; Perlepes, S. P.; Christou, G. *Dalton Trans.* **2007**, 3861–3863. (c) Stamatatos, T. C.; Diamantopoulou, E.; Raptopoulou, C. P.; Psycharis, V.; Escuer, A.; Perlepes, S. P. *Inorg. Chem.* **2007**, *46*, 2350–2352. (d) Aromi, G.; Bouwman, E.; Burzuri, E.; Carbonera, C.; Krzystek, J.; Luis, F.; Schlegel, C.; van Slageren, J.; Tanase, S.; Teat, S. J. *Chem.—Eur. J.* **2008**, *14*, 11158–11166. (e) Meally, S. T.; Karotsis, G.; Brechin, E. K.; Papaefstathiou, G. S.; Dunne, P. W.; McArdle, P.; Jones, L. F. *CrystEngComm* **2010**, *12*, 59–63.
(11) Annigeri, S. M.; Naik, A. D.; Gangadharmath, U. B.; Revankar, V. K.; Mahale, V. B. *Transition Met. Chem.* **2002**, *27*, 316–320.
(12) Bain, G. A.; Berry, J. F. *J. Chem. Educ.* **2008**, *85*, 532–536.
(13) *SAINT*, version 7.53a; Bruker Analytical X-ray Systems: Madison, WI, 2008.
(14) Sheldrick, G. M. *Acta Crystallogr., Sect. A* **2008**, *64*, 112–122.

Table 1. Crystal Data and Structure Refinement for Compounds **1**−**3**

	1	**2**	**3**
empirical formula	$C_{44}H_{63}ClDy_2N_6Ni_2O_{25}S_2$	$C_{44}H_{63}ClN_6Ni_2O_{25}S_2Tb_2$	$C_{44}H_{63}ClGd_2N_6Ni_2O_{25}S_2$
fw (g mol^{-1})	1617.99	1610.83	1607.49
cryst syst	orthorhombic	orthorhombic	orthorhombic
space group	$Pna2_1$	$Pna2_1$	$Pna2_1$
cryst color	brown	brown	brown
cryst size (mm^3)	0.19 × 0.15 × 0.12	0.19 × 0.17 × 0.14	0.19 × 0.17 × 0.14
temperature (K)	186(2)	186(2)	191(2)
a (Å)	14.3202(10)	14.3800(6)	14.3637(8)
b (Å)	26.7358(18)	26.6616(11)	26.6503(15)
c (Å)	14.9334(10)	14.9053(6)	14.9105(8)
V (Å^3)	5717.4(7)	5714.6(4)	5707.7(5)
ρ_{calcd} (Mg/m^3)	1.880	1.872	1.871
μ (mm^{-1})	3.439	3.301	3.151
F(000)	3224	3216	3208
θ for data collection (deg)	1.61−26.05	1.53−26.13	1.53−25.07
collected reflns	30 641	31 189	28 456
indep reflns	11 030	10 333	9986
R_{int}	0.0351	0.0478	0.0390
R [$I > 2\sigma(I)$]	0.0331	0.0340	0.0302
wR (all data)	0.0834	0.0868	0.0781
GOF on F^2	1.046	1.073	1.040
largest diff peak and hole (e Å^{-3})	1.166 and −1.324	0.937 and −0.555	1.031 and −0.504

contain the supplementary crystallographic data for this paper. These data can be obtained free of charge from the Cambridge Crystallographic Data Centre via www.ccdc.cam.ac.uk/data_request/cif. See also the Supporting Information.

Results and Discussion

Synthesis and Crystal Structures. The reaction of Ln(ClO$_4$)$_3$·6H$_2$O and Ni(OAc)$_2$·4H$_2$O with **H$_2$L** in methanol/acetone (2:1), in the presence of NaOH, produces brown crystals of [Ln$_2$Ni$_2$(μ_3-OH)$_2$(OH)(OAc)$_4$(HL)$_2$(MeOH)$_3$](ClO$_4$)·3MeOH [Ln = Dy (**1**), Tb (**2**), and Gd (**3**)]. **H$_2$L** is a versatile receptor able to adapt to the coordinative preferences of different metal ions. The "soft" nitrogen atoms of the ligand preferably coordinate "soft" metal ions; in contrast, the "hard" oxygen atoms rather bind to "hard" metal ions. According to hard−soft acid−base theory, the lanthanide ions are hard acids.[15] Consequently, it is expected that the ditopic ligand will coordinate the Ln^{III} ion through its oxygen atoms and bind the nickel ion through its nitrogen atoms. Therefore, the crucial use of this particular ligand, in principle, should allow control of the formation of the heterometallic coordination compounds.

The complexes are isostructural and crystallize in the orthorhombic space group $Pna2_1$ (Table 1). The structure of **2** is described here as representative of the whole series. The crystal structure consists of cationic entities [Tb$_2$Ni$_2$(μ_3-OH)$_2$(OH)(OAc)$_4$(HL)$_2$(CH$_3$OH)$_3$]$^+$, an uncoordinated perchlorate anion for charge balance, and methanol molecules of crystallization. A perspective view of the tetranuclear cations is depicted in Figure 1. The metal centers of the tetranuclear core are linked by two μ_3-phenoxido oxygen atoms from two HL$^-$ ligands and two μ_3-hydroxido groups to form a cubic arrangement of the metal ions and oxygen atoms. Two ligands bridge the Tb^{III} and Ni^{II} centers in an antiparallel fashion, with the O,O and N,N pockets coordinating to the Tb^{III} and Ni^{II} ions, respectively. The Tb^{III} and Ni^{II} ions are further bridged by acetates in a syn−syn μ−η^1:η^1 fashion to consolidate

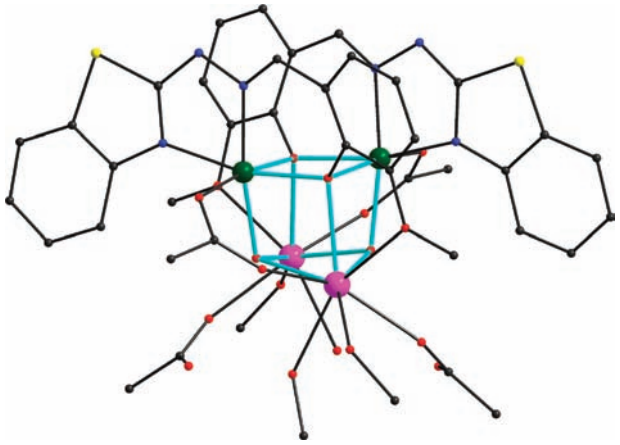

Figure 1. Structure of a [Tb$_2$Ni$_2$(μ_3-OH)$_2$(OH)(OAc)$_4$(HL)$_2$(CH$_3$OH)$_3$]$^+$ cation highlighting the [Tb$_2$Ni$_2$O$_4$] heterometallic cubane in turquiose lines. Hydrogen atoms are omitted for clarity. Color scheme: pink, Tb; green, Ni; red, O; blue, N; yellow, S; gray, C.

this heterometallic cubane. The coordination spheres of Tb1 and Tb2 are each completed by a monodentate acetate and two methanol molecules and a monodentate acetate, a hydroxyl group, and a methanol molecule, respectively, making them eight-coordinate with geometries between dodecahedral and bicapped trigonal prismatic. The protonation levels of OAc$^-$ and HO$^-$ ions were established by charge considerations and were evident from the presence of intramolecular hydrogen-bond interactions [O18−H18a···O8 = 3.030(7) Å; O16−H16b···O8 = 2.2.671(8) Å] and intermolecular hydrogen-bond interactions [O13−H13h···O8 = 2.612(8) Å; O19−H19···O16 = 2.696(9) Å].

Each Ni^{II} ion is in an elongated octahedral coordination environment. The basal plane of the octahedron is formed by two nitrogen atoms and one bridging phenoxido oxygen atom belonging to one HL$^-$ ligand and one oxygen atom from a bridiging hydroxido group. The axial positions are occupied by one acetate oxygen atom and the phenoxido oxygen atom of a second HL$^-$ ligand. The Ni−N and Ni−O bond lengths are in normal ranges for a NiN$_2$O$_4$ chromophore with an elongated octahedral

(15) Pearson, R. G. *J. Am. Chem. Soc.* **1963**, *85*, 3533–3539.

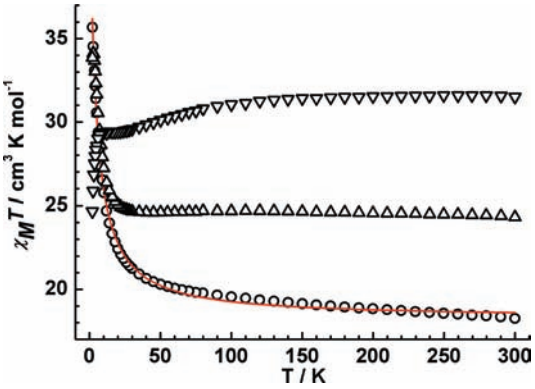

Figure 2. Temperature dependence of the $\chi_M T$ products at 1 kOe for **1** (▽), **2** (△), and **3** (○). The red line is the simulation of the experimental data.

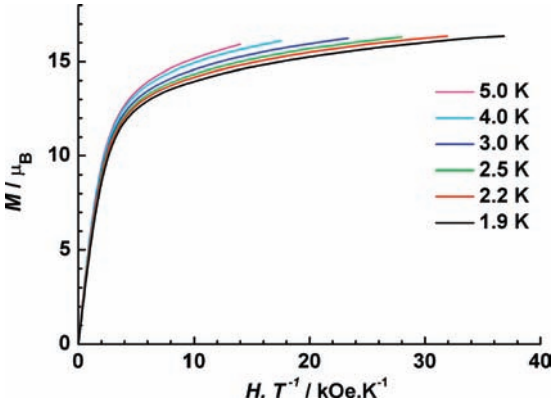

Figure 3. M vs H/T plots for **1** below 5 K.

geometry. This deformation of the cubane cluster is most likely due to steric constraints rising from its assembly. This $[Tb_2Ni_2]$ cubane is reminiscent of the substructures reported in the $[Dy_3Cu_6]$ cluster[4] with a Ni···Ni separation of 3.2751(12) Å, a Tb···Tb separation of 3.8805(4) Å, and Tb···Ni distances in the range of 3.3952(10)−3.5866(9) Å. These cubane compounds provide unique opportunities to allow for a systematic exploration of features that have been identified as being important in shedding light on the SMM behavior encountered in the $[Dy_3Cu_6]$ cluster.[4]

Magnetic Properties. dc magnetic susceptibility studies of **1**−**3** were carried out in an applied magnetic field of 1 kOe over the temperature range 2−300 K. The plots of $\chi_M T$ versus T, where χ_M is the molar magnetic susceptibility, are shown in Figure 2. For **1**, the observed $\chi_M T$ value of 31.5 cm^3 K mol^{-1} is close to the expected value of 30.3 cm^3 K mol^{-1} for two uncoupled Dy^{III} ions ($^6H_{15/2}$, $S = {}^5/_2$, $L = 5$, $J = {}^{15}/_2$, and $g = {}^4/_3$) and two uncoupled Ni^{II} ions ($S = 1$ and $g = 2$). The $\chi_M T$ product gradually decreases upon lowering of the temperature, reaching a plateau of 29.4 cm^3 K mol^{-1} at 20 K, and then drops further to a minimum value of 24.7 cm^3 K mol^{-1} at 2 K. For **2**, at room temperature, the $\chi_M T$ value of 24.7 cm^3 K mol^{-1} is close to the expected value of 25.6 cm^3 K mol^{-1} for two uncoupled Tb^{III} ions ($^7F_6$, $S = 3$, $L = 3$, $J = 6$, and $g = {}^3/_2$) and two uncoupled Ni^{II} ions ($S = 1$ and $g = 2$). The $\chi_M T$ product gradually increases upon lowering of the temperature until 50 K and then increases sharply to a maximum value of 33.9 cm^3 K mol^{-1} at 2 K. This increase of $\chi_M T$ at low temperature may suggest the presence of intramolecular ferromagnetic interactions within the metal cubane. However, it is difficult to comment on the interactions of Ni···Ln and Ln···Ln in **1** and **2**, with lanthanide ions having intrinsic complicated magnetic characteristics, which include the presence of spin−orbit coupling and magnetic anisotropy.[8]

In **3**, the introduction of magnetically isotropic Gd^{III} ions allows us to estimate the magnetic interactions of Ni···Gd and Ni···Ni. Thus, their study seems crucial for the understanding of systems containing anisotropic lanthanide ions such as dysprosium and terbium, whose magnetic properties are much more complicated to understand. For **3**, at room temperature, the $\chi_M T$ value of 18.3 cm^3 K mol^{-1} is in good agreement with the expected value of 17.8 cm^3 K mol^{-1} for two uncoupled Gd^{III} ions ($^8S_{7/2}$, $S = {}^7/_2$, and $g = 2$) and two noninteracting Ni^{II} ions ($S = 1$ and $g = 2$). The $\chi_M T$ product gradually increases upon lowering of the temperature until 50 K and then increases sharply to a maximum value of 35.7 cm^3 K mol^{-1} at 2 K. This increase of $\chi_M T$ at low temperature obviously suggests the presence of intramolecular ferromagnetic interactions within the metal cubane.[16] To gain some information concerning the interactions between the metal ions within the cubane, as a preliminary treatment, the experimental magnetic data are analyzed based on a simple parallelogram model (Figure S1 in the Supporting Information),[17] where J_1, J_2, and J_3 represent the exchange interactions between Ni···Gd, Ni···Ni, and Gd···Gd, respectively. By assuming that $J_3 = 0$, the Heisenberg spin Hamiltonian is thus given as $H = -2J_1(S_{Ni1}S_{Gd1} + S_{Gd1}S_{Ni2} + S_{Ni2}S_{Gd2} + S_{Gd2}S_{Ni1}) - 2J_2S_{Ni1}S_{Ni2}$. The best fitting of the susceptibility data in terms of the Kambe model[18] in the temperature range 2−300 K gives $J_1 = 0.919$ cm^{-1}, $J_2 = -3.638$ cm^{-1}, $g = 2.03$, and $R^2 = 0.997\,51$. The results indicate that a ferromagnetic interaction between nickel and gadolinium ions and an antiferromagnetic interaction between two nickel ions are operative.

Magnetization (M) data for **1**−**3** were collected in the 0−70 kOe field range below 5 K. For **1** and **2**, the M versus H/T (Figures 3 and S2 in the Supporting Information) data at different temperatures show nonsuperposition plots, and a gradual increase of the magnetization at low fields, without a clear saturation even at 7 T, indicates the presence of a significant magnetic anisotropy and/or low-lying excited states.[19]

For **3**, the magnetization measurements at 1.9 K (Figure 4) show a clear saturation above 4 T indicative of a low magnetic anisotropy, which is further confirmed by the M versus H/T plot, where the data can almost be superposed on a single master curve, as is expected for isotropic systems (Figure S3 in the Supporting Information).[16] It is worth noting that, for the lower fields, the magnetization is above the magnetization calculated with the Brillouin function for two uncoupled $S = {}^7/_2$ and two

(16) Wu, G.; Hewitt, I. J.; Mameri, S.; Lan, Y.; Clérac, R.; Anson, C. E.; Qiu, S.; Powell, A. K. *Inorg. Chem.* **2007**, *46*, 7229–7231.
(17) Kahn, O. *Molecular Magnetism*; Wiley-VCH: New York, 1993.
(18) Kambe, K. *J. Phys. Soc. Jpn.* **1950**, *5*, 48–51.
(19) Lin, P.-H.; Burchell, T. J.; Ungur, L.; Chibotaru, L. F.; Wernsdorfer, W.; Murugesu, M. *Angew. Chem., Int. Ed.* **2009**, *48*, 9489–9492.

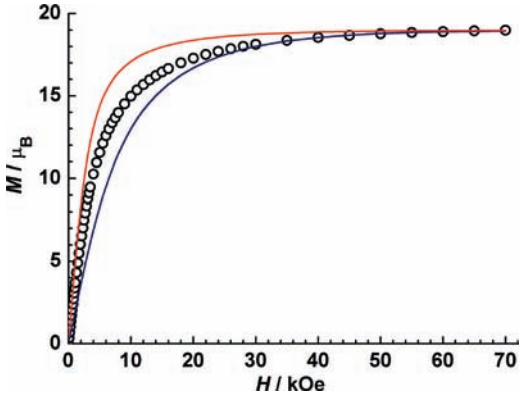

Figure 4. M vs H plot for **3** at 1.9 K (open cycle), Brillouin curves for $S = 9$ (red line), and uncoupled $^7/_2 + ^7/_2 + 1 + 1$ spins (navy line).

uncoupled $S = 1$ spin centers but below the magnetization calculated with the Brillouin function for $S = 9$ (Figure 4), which is consistent with the results that ferromagnetic Gd···Ni exchange interactions are competing with antiferromagnetic Ni···Ni interactions in the metal cubane.

ac susceptibility measurements were carried out for **1**−**3** under a zero dc field to investigate the dynamics of the magnetization. Compounds **2** and **3** do not exhibit any slow magnetic relaxation, as was confirmed by the lack of an out-of-phase ac signal (Figures S4 and S5 in the Supporting Information).[16] Strikingly, a frequency-dependent increase of the in-phase signal, together with the concomitant appearance of an out-of-phase signal, is observed for **1**, indicating the onset of slow magnetization relaxation, which is typical for SMM behavior (Figure S6 in the Supporting Information). Although the ac susceptibility as a function of the temperature does not show any peak in the out-of-phase ac susceptibility in zero dc field, it is strongly affected by a small dc field, highlighting the presence of fast quantum tunneling of magnetization, which can be significantly slowed down by the applied field.[20] Indeed, the peak in the out-of-phase ac susceptibility is observed under a 1200 Oe dc field for higher frequencies, as shown in Figure S7 in the Supporting Information.

To further probe the dynamics of this system, ac susceptibility measurements as a function of the frequency at different temperatures under a 1200 Oe dc field were carried out. The relaxation time at different temperatures was extracted by fitting the χ'' versus frequency curves (Figure 5).[21] Plotting the relaxation time versus the reciprocal temperature afforded the Arrhenius plot in Figure S8 in the Supporting Information. Above 2.3 K, the relaxation follows a thermally activated mechanism with an energy gap of 7.6 K and a preexponential factor, τ_0, of about 7.5×10^{-6} s. Because no out-of-phase signal was detected for the analogue **3**, it was found that the magnetic slow-relaxation behavior of complex **1** arises mainly from the presence of anisotropic Dy^{III} ions, as is observed in the Co_2Dy_2 system[8] and in a 3d−4f cluster

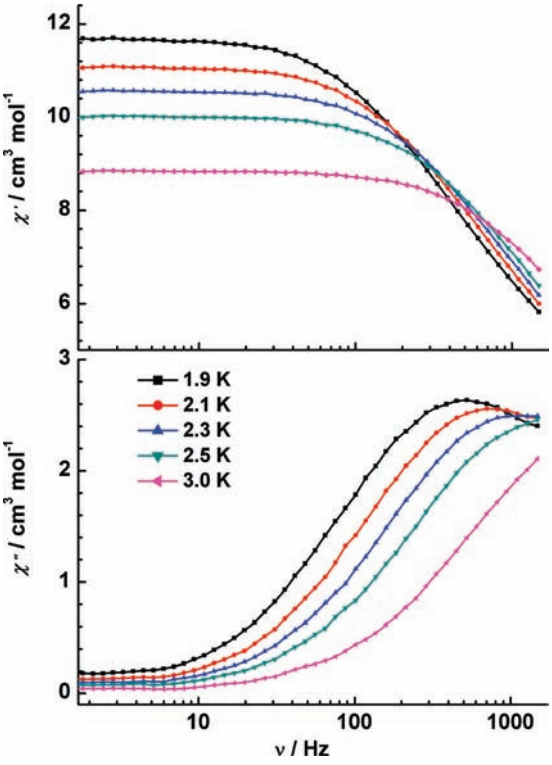

Figure 5. Frequency dependence of the in-phase (χ') and out-of-phase (χ'') parts of the ac susceptibility for **1** under a 1200 Oe dc field.

having a free Dy^{III} ion.[22] Nevertheless, the intramolecular magnetic interactions as a secondary consideration may also mediate the magnetic relaxation of 4f-based magnetic clusters.[23]

Concluding Remarks

In summary, three new heterometallic compounds containing $[Ln_2Ni_2O_4]$ cubane clusters have been prepared by using ditopic Schiff-base ligand $\mathbf{H_2L}$, capable of both coordinating and connecting 3d and 4f metal ion centers. ac susceptibility measurements on **1** reveal a frequency-dependent out-of-phase signal, indicative of slow relaxation of magnetization, which can be significantly slowed down by the application of a dc field, highlighting the presence of a fast zero-field relaxation of magnetization. Magnetic analysis on compound **3** indicates ferromagnetic Gd···Ni exchange interactions competing with antiferromagnetic Ni···Ni interactions. This synthetic approach may represent a promising new route toward the design of new heterometallic clusters and novel magnetic materials.

Acknowledgment. We thank the National Natural Science Foundation of China (Grants 20761004, 20871113, and 91022009) for financial support.

Supporting Information Available: Crystallographic data in CIF format and additional magnetic data for compounds **1**−**3**. This material is available free of charge via the Internet at http://pubs.acs.org.

(20) Ako, A. M.; Mereacre, V.; Hewitt, I. J.; Clerac, R.; Lecren, L.; Anson, C. E.; Powell, A. K. *J. Mater. Chem.* **2006**, *16*, 2579–2586.
(21) Poneti, G.; Bernot, K.; Bogani, L.; Caneschi, A.; Sessoli, R.; Wernsdorfer, W.; Gatteschi, D. *Chem. Commun.* **2007**, 1807–1809.
(22) Nayak, S.; Roubeau, O.; Teat, S. J.; Beavers, C. M.; Gamez, P.; Reedijk, J. *Inorg. Chem.* **2009**, *49*, 216–221.
(23) Pointillart, F.; Bernot, K.; Sessoli, R.; Gatteschi, D. *Chem.—Eur. J.* **2007**, *13*, 1602–1609.